Research Square

Preprints are preliminary reports that have not undergone peer review.
They should not be considered conclusive, used to inform clinical practice,
or referenced by the media as validated information.

A 26-year satellite record of vegetation phenology and productivity proxy across Europe

Hongxiao Jin

Hongxiao.jin@mgeo.lu.se

Lund University

Zhanzhang Cai

Lund University

Astrid Vannoppen

Flemish Institute for Technological Research (VITO)

Dominique Munck

Flemish Institute for Technological Research (VITO)

Else Swinnen

Flemish Institute for Technological Research (VITO)

Walter Horsten

Flemish Institute for Technological Research (VITO)

Wai-Tim Ng

Flemish Institute for Technological Research (VITO)

David Bekaert

Flemish Institute for Technological Research (VITO)

Luca Battistella

European Environment Agency (EEA)

Ludvig Forslund

European Environment Agency (EEA)

Eva Ivits

Eurostat

Jonas Ardö

Lund University

Lars Eklundh

Lund University

---

data-descriptor

Keywords:

Posted Date: November 12th, 2026

DOI: https://doi.org/10.21203/rs.3.rs-11340886/v1

License: This work is licensed under a Creative Commons Attribution 4.0 International License.
Read Full License

Additional Declarations: No competing interests reported.

A 26-year satellite record of vegetation phenology and productivity proxy across Europe

Hongxiao Jin (靳洪晓)[1,*]; Zhanzhang Cai (蔡展章)[1], Astrid Vannoppen[2], Dominique De Munck[2], Else Swinnen[2], Walter Horsten[2], Wai-Tim Ng[2], David Bekaert[2], Luca Battistella[3], Ludvig Forslund[3], Eva Ivits[4], Jonas Ardö[1], Lars Eklundh[1]

[1] Department of Earth and Environmental Sciences, Lund University, Lund, Sweden.

[2] Flemish Institute for Technological Research (VITO), Mol, Belgium,

[3] European Environment Agency (EEA), Copenhagen K, Denmark

[4] European Commission, Eurostat, Luxembourg.

* Corresponding author: Hongxiao Jin, Hongxiao.jin@mgeo.lu.se

Abstract

Satellite land surface phenology describes seasonal vegetation development across landscapes. We present MR-VPP 5.0, a 26-year record (2000–2025) of vegetation phenology and seasonal productivity proxy across Europe, available through Copernicus Land Monitoring Service (CLMS). The dataset is derived from MODIS Collection 6.1 NBAR reflectance, contains 13 annual vegetation phenology and productivity (VPP) metrics for up to two growing seasons per year, Plant Phenology Index (PPI) seasonal trajectories at 5-day interval, and quality information, on a 500 m ETRS89-LAEA grid. VPP metrics describe the timing and magnitude of green-up, seasonal maximum and senescence, season length, rates of change, and integrated PPI. Quality-weighted daily PPI observations were processed with TIMESAT Version 4.2 to reconstruct seasonal curves and identify growing seasons. Technical checks examine processing artefacts, output quality and the consistency of the 2025 annual-update strategy against full-archive processing, and temporal correspondence with documented disturbances. The record supports regional and continental studies of vegetation seasonality, ecosystem productivity, and responses to climate variability and disturbance.

Background & Summary

Vegetation phenology describes the recurring seasonal development of plant and their responses to climate, disturbance and management[1]. Satellite observations extend phenological monitoring beyond individual organisms and sites by tracking seasonal changes in vegetation across landscapes. This land surface phenology characterizes vegetation dynamics within each pixel and reflects collective expression of individual events such as budburst or leaf falling[2-5]. Long records processed with consistent methods provide a basis for examining interannual variability, responses to extreme events and changes in canopy development[6-8].

The Medium Resolution Vegetation Phenology and Productivity Version 5.0 Issue 2.0 (MR-VPP 5.0), was released through Copernicus Land Monitoring Services in August 2026 [9]. It is the first release of the product for public access since the MR-VPP mission started in 2019. MR-VPP provided the vegetation-productivity information used in the European Environment Agency's drought impact on ecosystems indicator[10,11]. MR-VPP 5.0 is a 26-year record covering 2000–2025 across the pan-European domain. The dataset is derived from MODIS Collection 6.1 Nadir Bidirectional Reflectance Distribution Function (BRDF) Adjusted Reflectance (NBAR) and distributed on a 500m ETRS89-LAEA Europe grid.

The Plant Phenology Index (PPI)[12] provides the basis for MR-VPP. PPI is a dimensionless, physically based vegetation index derived from a canopy radiative-transfer model using red and near-infrared (NIR) reflectance. It was developed to track canopy development with an approximately linear response to photosynthetically effective green leaf area and has shown close agreement with seasonal variations in gross primary productivity in boreal forests and other vegetation cover types[12-15]. This physical basis supports interpretation of seasonal changes in photosynthetically effective foliage and motivates its use for retrieving phenology and seasonal productivity indicators across Europe.

The dataset contains two complementary components: seasonal trajectories (ST) at 5-day intervals and 13 annual vegetation phenology and productivity (VPP) metrics for up to two detected growing seasons per year, with accompanying quality information. ST describes vegetation development within and across calendar years, allowing users to examine interannual anomalies, interruptions and subsequent recovery. These trajectories support vegetation response to drought stress[6] and provide temporal framework for studying differences in seasonal timing among habitats and potential trophic and reproduction mismatches[16] in relatively high resolution over continental scale. VPP summarizes each detected season through its timing, magnitude, duration, rates of change and integrated PPI. Users are therefore able to compare annual metrics while retaining access to the trajectories from which they were derived. Integrated PPI provides an indicator for seasonal productivity dynamics and can support studies of seasonal aggregated vegetation responses to climatic stress. Because it is derived without explicit climate forcing, it reduces the risk of circular reasoning that can arise when relating climate variables to satellite-derived primary productivity estimates modelled using those same variables. It also avoids biases in vegetation productivity estimates due to insufficiently handling of climate stresses in model[17].

Version 5.0 incorporates daily processing inputs, revised treatment of bright sparsely vegetated surfaces, updated quality information and TIMESAT 4.2 [18] for trajectory reconstruction and metric extraction. This descriptor documents the released record, evaluates its technical quality and provides guidance for regional and continental analyses of vegetation seasonality and productivity.

Methods

The processing methods are summarized below. Full equations, implementation details and quality definitions are provided in the MR-VPP 5.0 Algorithm Theoretical Basis Document (ATBD, Sections 2–4)[19] and the accompanying Product User Manual (PUM, Section 3)[20].

Input satellite observations

Daily MODIS Collection 6.1 MCD43A4 NBAR and MCD43A2 quality data were obtained from NASA's Level-1 and Atmosphere Archive and Distribution System (LAADS) Distributed Active Archive Center (DAAC). MCD43A4 supplies reflectance normalized to nadir view at local solar noon using the Ross-Thick-Li-Sparse Reciprocal BRDF model[21]. Although values are provided daily, each retrieval draws on observations within a 16-day moving window, resulting relatively smooth daily time series. For this reason, we retain the original 5-day PPI seasonal trajectory in the product release to preserve temporal detail while limiting storage requirements. MCD43A2 provides band-specific retrieval quality and ancillary information used to weight PPI observations. Twenty-three MODIS sinusoidal tiles (h15v05, h16v02, h16v05–v06, h17v02–v05, h18v01–v06, h19v01–v05, h20v03–v05, and h21v04–v05) cover the processing domain, which comprises the EEA-39 area and the part of Ukraine.

The full input archive extended from 24 February 2000 to 19 April 2026, providing temporal context beyond the final product year. This temporal buffer beyond the final product year supports estimation of seasons whose decline extends into early 2026. The operational 2025 update used a shorter window from 1 January 2024 to19 April 2026, for examine its agreement with full-archive processing. This examination is particularly relevant for future VPP updating, which usually use a short input data window instead of full time series to reduce computation costs.

PPI calculation and observation quality

Daily PPI was calculated using the physically based formulation of Jin and Eklundh [12]:

$$PPI = -K \cdot ln\frac{MDVI-DVI}{MDVI-DVI_S}, \quad (1)$$

where DVI is the difference between NIR and red reflectance, MDVI is its long-term potential maximum, DVI_s represents the soil background, and K accounts for canopy light extinction and illumination geometry. PPI represents photosynthetically effective green leaf area and is expressed in $m^2 \cdot m^{-2}$, an area ratio that is dimensionless as LAI. PPI is approximately linearly related to green LAI, although their numerical relationship depends on canopy properties and model assumptions. MDVI was estimated for each pixel from the long MODIS record, with a lower bound of 0.18. The definition of DVI_s and K are given in ATBD Section 2.2.

In MR-VPP 5.0, PPI values were restricted to −1 to 5 m^2 m^{-2}. Values below or above this range were truncated and identified in the PPI quality layer. Observations with both red reflectance > 0.35 and DVI > 0.05 were assigned PPI = 0 to suppress bright-soil artefacts. This treatment was introduced because seasonal reflectance variation over bright barren surfaces can otherwise be propagated into false vegetation seasons. Corrections and invalid observations were recorded in the PPI quality layer.

PPI quality was derived from the MCD43A2 quality of red and NIR bands, with respective contributions of 0.1 and 0.9. Good, fair, poor and unusable PPI observations received fitting weights of 1.0, 0.6, 0.1 and 0, respectively, in the subsequent TIMESAT processing. Diagnostic PPI quality codes identify truncation, bright-soil correction, invalid PPI and missing observations.

PPI trajectory fitting and seasonal metrics extraction

Quality-weighted daily PPI series were processed with TIMESAT Version 4.2 [22,23]. Pre-processing established a local base level, incorporated observation weights, treated long temporal gaps and identified coarse candidate seasons. Cubic smoothing spline was fitted to reconstruct a daily seasonal trajectory using a smoothing parameter of 1000. The algorithm then identified local minima and maxima and retained seasons that met minimum duration, amplitude and data-quality requirements.

The start and end of season were defined at 25% and 15% of the fitted seasonal amplitude on the rising and declining phases, respectively. The remaining metrics were then derived from the fitted trajectory. Up to two seasons were stored for each product year. When more than two candidate seasons were detected, the two with the highest peak PPI values were retained and labelled chronologically. A subsequent amplitude-ratio criterion could remove the weaker of these seasons.

A growing season was assigned to the calendar year containing its maximum-of-season date. Consequently, its start may fall in the preceding year and its end may fall in the following year. Date values retain this temporal information: SOSD may be negative for a season starting before 1 January of the assigned year, while EOSD may exceed 365 or 366 for a season ending in the following year. This convention avoids splitting a continuous vegetation cycle at an arbitrary calendar boundary.

The fitted trajectory yielded 13 metrics describing dates of season start, maximum and end; PPI values at these dates; the mean of the two bounding minima; seasonal amplitude; season length; rates of increase and decrease; and two integrals (Table 1). Total productivity is the integral of the fitted daily PPI between start and end. Seasonal productivity is the corresponding integral above the season-specific base level.

Quality assessment and outputs

Retrieval quality is assessed separately for green-up, peak and green-down using the number and mean quality of valid PPI observations and then combined into an overall season-quality class (Figure 1). A

one-byte quality value accompanies every VPP metric for each season. The lower six bits encode the three two-bit phase classes, and the two most significant bits encode overall season quality. Each two-bit class ranges as 0– best, 1– good, 2– fair, and 3– poor. A practical first-order screen is QA < 127, which identifies retrievals with no more than one poor-quality phase. QA = 255 denotes failure or no retrieval and must be excluded.

MODIS Tile-based outputs were mosaicked, reprojected to ETRS89-LAEA Europe (EPSG:3035) and resampled to the 500 m grid. Nearest-neighbor resampling preserved the integer-coded dates, quality values and stored metric values. Products are distributed as Cloud-Optimized GeoTIFF rasters with lossless compression. Separate files are provided for every metric, product year and detected season.

Table 1. Annual MR-VPP parameters. All metric rasters use INT16 format and -9999 as the fill value; QA uses byte format and 255 as the fill value.

Parameter	Definition	Unit	Physical range	Scale factor
SOSD	Start-of-season date	day of year	−365 to 365	1
EOSD	End-of-season date	day of year	0 to 730	1
MAXD	Date of seasonal maximum	day of year	0 to 366	1
SOSV	PPI at SOSD	$m^2\ m^{-2}$	0 to 5	0.001
EOSV	PPI at EOSD	$m^2\ m^{-2}$	0 to 5	0.001
MINV	Mean PPI of the two season-bounding minima	$m^2\ m^{-2}$	0 to 5	0.001
MAXV	PPI at MAXD	$m^2\ m^{-2}$	0 to 5	0.001
AMPL	Seasonal amplitude, MAXV − MINV	$m^2\ m^{-2}$	0 to 5	0.001
LENGTH	Number of days between SOSD and EOSD	day	0 to 730	1
LSLOPE	Rate of PPI increase during green-up	$m^2\ m^{-2}\ day^{-1}$	0 to 1	0.001
RSLOPE	Absolute rate of PPI decrease during green-down	$m^2\ m^{-2}\ day^{-1}$	0 to 1	0.001
TPROD	Integral of fitted PPI from SOSD to EOSD	$m^2\ m^{-2}$ day	0 to 2000	1
SPROD	Integral of fitted PPI above the seasonal base level	$m^2\ m^{-2}$ day	0 to 2000	1
QA	Season-specific retrieval-quality bit field	–	0 to 255	–

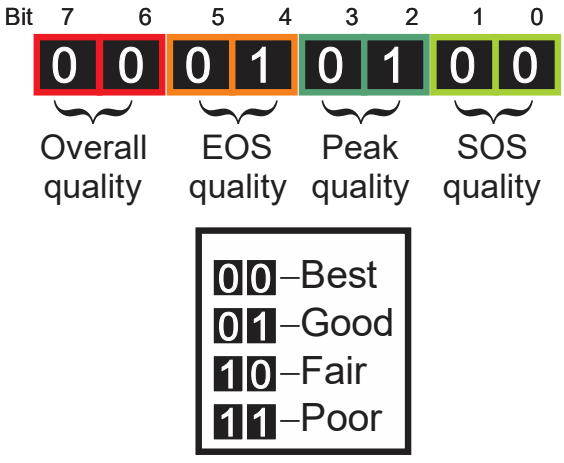


Figure 1. Structure of the eight-bit VPP quality field. Two bits describe each of the start, peak and end phases, and the two most significant bits describe overall season quality. Example: QA=00010100

147 (20) means an overall best phenology retrieval, with best quality for SOS, good quality for peak and
148 EOS estimations.

149 ## Data Records

150 MR-VPP 5.0 is distributed through the Copernicus Land Monitoring Service (CLMS). Figure 2 shows
151 the product's spatial coverage, illustrated by Season 1 total productivity (TPROD) of 2025. PPI, VPP
152 and their respective quality layers are available through separate catalogue pages (Table 2).

153 **Table 2.** Catalogue and download access points for MR-VPP 5.0 products.

Component	CLMS catalogue	Access point and Digital Object Identifier (DOI)
PPI time series	Plant Phenology Index, 5-daily	https://land.copernicus.eu/en/products/vegetation/medium-resolution-plant-phenology-index-2000-2025-raster-500-m-europe-5-daily https://doi.org/10.2909/9db29b07-5968-4ce0-8351-1e356b3d7d47
PPI quality	Plant Phenology Index Quality Flag, 5-daily	https://land.copernicus.eu/en/products/vegetation/medium-resolution-plant-phenology-index-quality-flag-2000-2025-raster-500-m-europe-5-daily https://doi.org/10.2909/e9c725f4-f624-476f-8304-8d3c3b8e2d2d
VPP metrics	Vegetation Parameters, yearly	https://land.copernicus.eu/en/products/vegetation/medium-resolution-vegetation-parameters-2000-2025-raster-500-m-europe-yearly End-of-Season Date DOI: https://doi.org/10.2909/998c06c6-6abf-479d-9b99-7023598409e4 End-of-Season Value DOI: https://doi.org/10.2909/6b394b30-fddc-40d1-b70d-fe047c61da99 Season Amplitude DOI: https://doi.org/10.2909/e96c138d-2ca5-43c0-a3c8-c27ef8555e14 Season Length DOI: https://doi.org/10.2909/52939031-5f8f-47ba-ba62-f57566baa4aa Season Maximum Date DOI: https://doi.org/10.2909/2b5348ac-d6ce-49e6-92a6-a3a6252b8826 Season Maximum Value DOI: https://doi.org/10.2909/4c1635a6-2498-45e0-8765-893d9c43312b

		Season Minimum Value DOI: https://doi.org/10.2909/51290962-3beb-4bac-bd06-0997de245949 Seasonal Productivity DOI: https://doi.org/10.2909/d3919020-1b88-4c39-a6dc-f78a5d1af114 Total Productivity DOI: https://doi.org/10.2909/b44bea25-62ce-4549-ad8c-a62bc39e9d86 Start-of-Season Date DOI: https://doi.org/10.2909/39d1a37f-d864-4b5a-b94f-2b54930e45d7 Start-of-Season Value DOI: https://doi.org/10.2909/181c3a99-a2ee-4118-9c88-b7dfa5e23f8d Slope of the Green-down Period DOI: https://doi.org/10.2909/e9a7a89e-f0a8-4dbe-aa22-141ef0e164ab Slope of the Green-up Period DOI: https://doi.org/10.2909/7413d030-d782-4dd9-a6e0-d42db6c6b06e
VPP quality	Vegetation Parameters Quality Flag, yearly	https://land.copernicus.eu/en/products/vegetation/medium-resolution-vegetation-parameters-quality-flag-2000-2025-raster-500-m-europe-yearly https://doi.org/10.2909/990ea9d2-5678-462a-91e3-2f38dae0f77c

Note: Appending #download to a catalogue URL opens its download tab. E.g. *https://land.copernicus.eu/en/products/vegetation/medium-resolution-plant-phenology-index-2000-2025-raster-500-m-europe-5-daily*#download

PPI time series trajectories (ST)

The PPI time-series archive provides the vegetation-index observations used as input to phenology retrieval, sampled at nominal 5-day intervals. Sampling dates are the 1st, 6th, 11th, 16th, 21st and 26th of each month, giving 72 dates per complete year. This sampling supports analyses of seasonal vegetation dynamics while reducing storage and download volumes. The dates also align with the nominal 10-day schedule of other CLMS products, including NDVI[24], through selection of the 1st, 11th and 21st of each month.

PPI is stored as a signed 16-bit integer with a scale factor of 0.001, zero offset and a fill value of 32767. Stored values from −1000 to 5000 correspond to −1 to 5 m^2 m^{-2}. Filenames follow PPI.YYYY.MM.DD.laea.cog.tif and QA.YYYY.MM.DD.laea.cog.tif for PPI and its quality information respectively. PPI files are grouped into yearly ZIP archives, approximately 6 GB each; corresponding quality layers are downloaded separately.

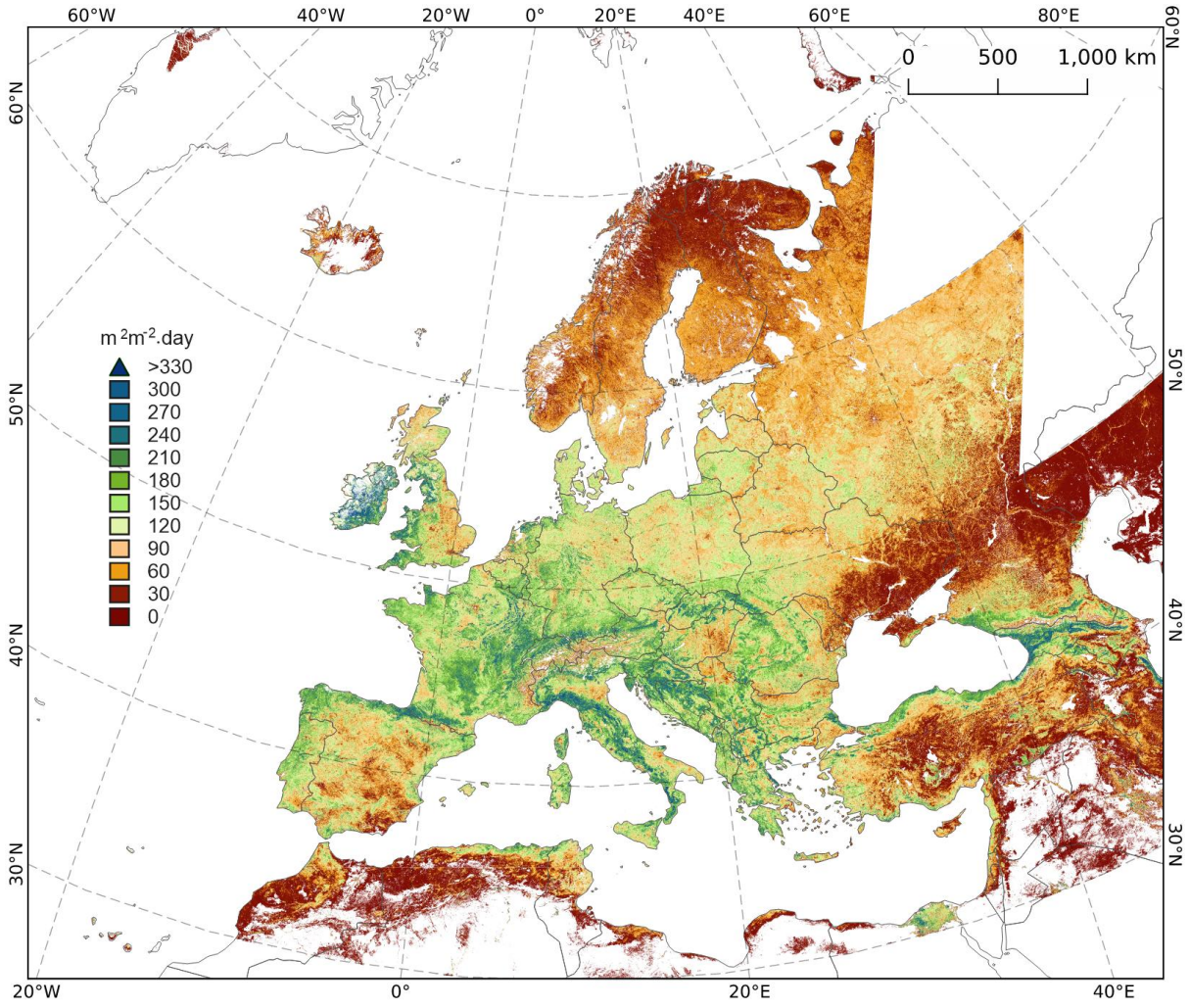


Figure 2. Spatial coverage of MR-VPP 5.0, illustrated by Season 1 total productivity (TPROD) for 2025. TPROD is the sum of fitted daily PPI values between the start and end of the season (SOSD and EOSD), expressed in $m^2\ m^{-2}$ day. Only pixels with QA < 127 (Best or Good quality) are displayed; pixels with missing TPROD values or QA > 127 are left uncolored.

PPI quality is stored as an unsigned eight-bit integer. Codes 0–1 indicate good quality, 2 fair quality and 3–253 poor quality or diagnostic conditions. Diagnostic codes identify DVI exceeding MDVI (250), upper and lower PPI truncation (251 and 252), bright-soil correction (253), invalid PPI (254) and missing observations (255). These observation-level codes differ from the season-level VPP quality encoding.

Annual VPP metrics

The VPP archive contains 13 metrics and one associated quality layer for each of up to two retained growing seasons per product year. Each metric is supplied in a separate raster. VPP filenames follow the pattern PARAMETER_YYYY_SEASON_cog.tif, where SEASON is season1 or season2; for example, TPROD_2025_season1_cog.tif contains Season 1 TPROD of 2025. Corresponding quality files follow the same convention, with QA replacing the parameter code.

The product year is the year containing the seasonal maximum; season start and end dates may therefore fall in the preceding or following calendar year. Parameters definitions, units, ranges and scale factors are listed in Table 1. VPP metrics are stored as signed 16-bit integers with a fill value of −9999. VPP quality is stored as an unsigned eight-bit integer, with 255 indicating retrieval failure or missing output.

Data Overview

Figures 3 and 4 summarize spatial and temporal variation in Season 1 TPROD across Europe during 2000–2025. Both calculations excluded raster NoData values (−9999), required at least 20 valid annual observations per pixel. Trends were estimated using pixelwise Theil–Sen slopes. Annual anomalies were calculated by subtracting the mean trend residual from each annual residual and dividing by the sample standard deviation of the residuals. Pixels with a non-finite residual standard deviation or a residual standard deviation $\leq 10^{-6}$ were excluded from the anomaly outputs and from the stored trend and Mann–Kendall products. Negative anomalies indicate lower seasonal integrated vegetation activity relative to each pixel's detrended baseline. Documented European droughts, for example, in 2003 and 2015 provide independent context[25,26], likely explained the negative anomalies in corresponding European areas in Figure 3, but the causes of the mapped anomalies and trends were not further investigated.

Positive slopes are widespread, whereas negative slopes occur in more localized patches (Figure 4). These patterns describe changes in seasonal integrated vegetation activity; likely associated with carbon uptake. However, their environmental and management drivers need further investigation. Trend significance was assessed using the standard Mann–Kendall test at a nominal threshold of $p \leq 0.05$, without correction for temporal autocorrelation or multiple testing across pixels. For readability, significance symbols are shown only at sampled locations on a regular grid with approximately 50 km spacing. They indicate local, unadjusted significance at those locations.

Technical Validation

We examine processing artefacts, the consistency of annual updates, and the PPI time-series responses to documented disturbances, including droughts, insect outbreaks, and wildfires. These assessments illustrate the potential of MR-VPP for monitoring vegetation dynamics and do not constitute independent validation against field observations of phenology or productivity. Previous evaluations of PPI and PPI-derived phenology, as well VPP processing algorithms using TIMESAT, can be found in e.g.[12,27].

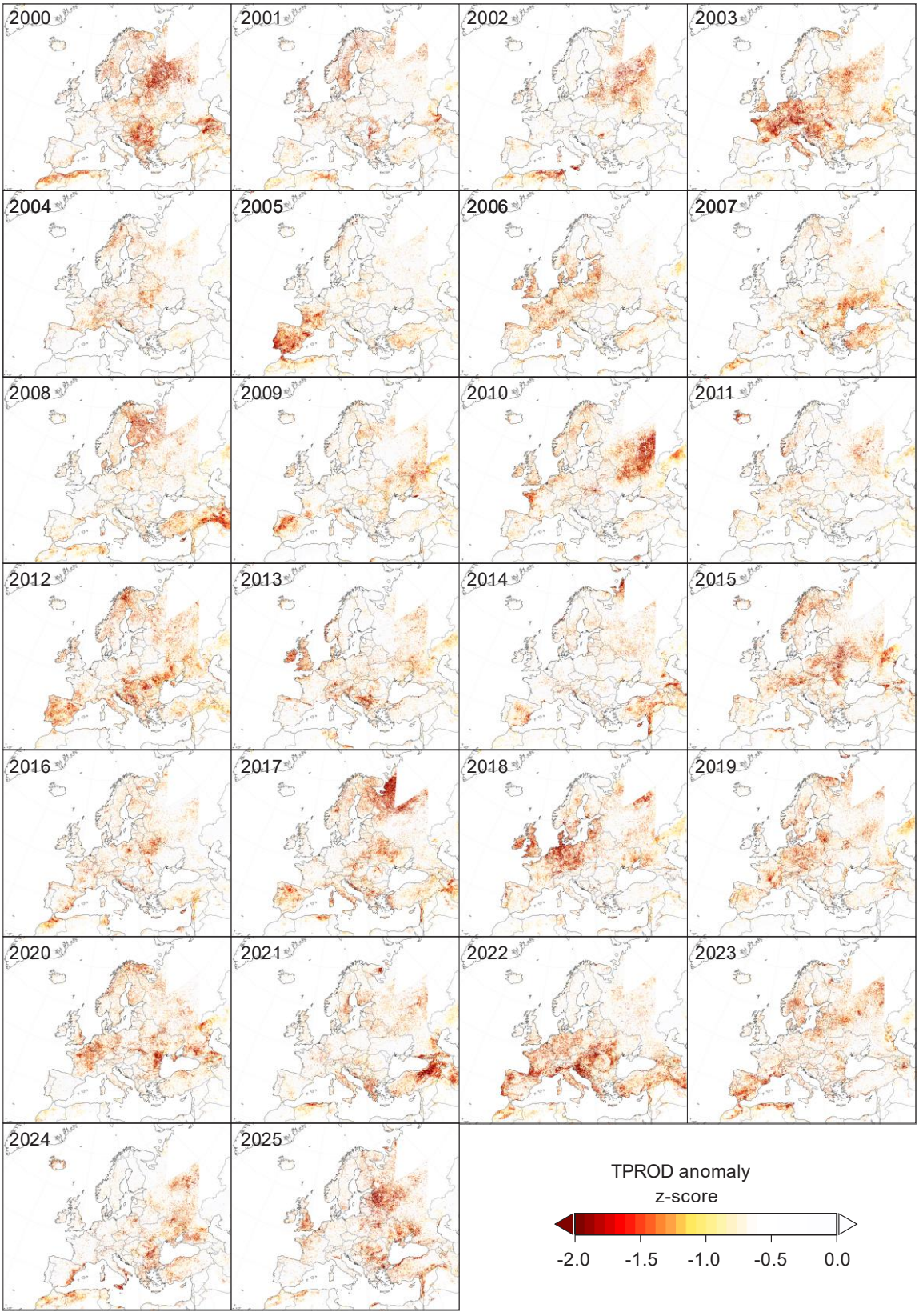


Figure 3. Standardized annual anomalies in Season 1 total productivity (TPROD) across Europe, 2000–2025, derived from the 500 m MODIS-based MR-VPP 5.0 record. At each pixel, residuals from a linear Theil–Sen trend were centered and divided by their sample standard deviation. Negative z-scores are shown using a fixed color range of −2 to 0, with values ≤ −2 displayed in dark red.

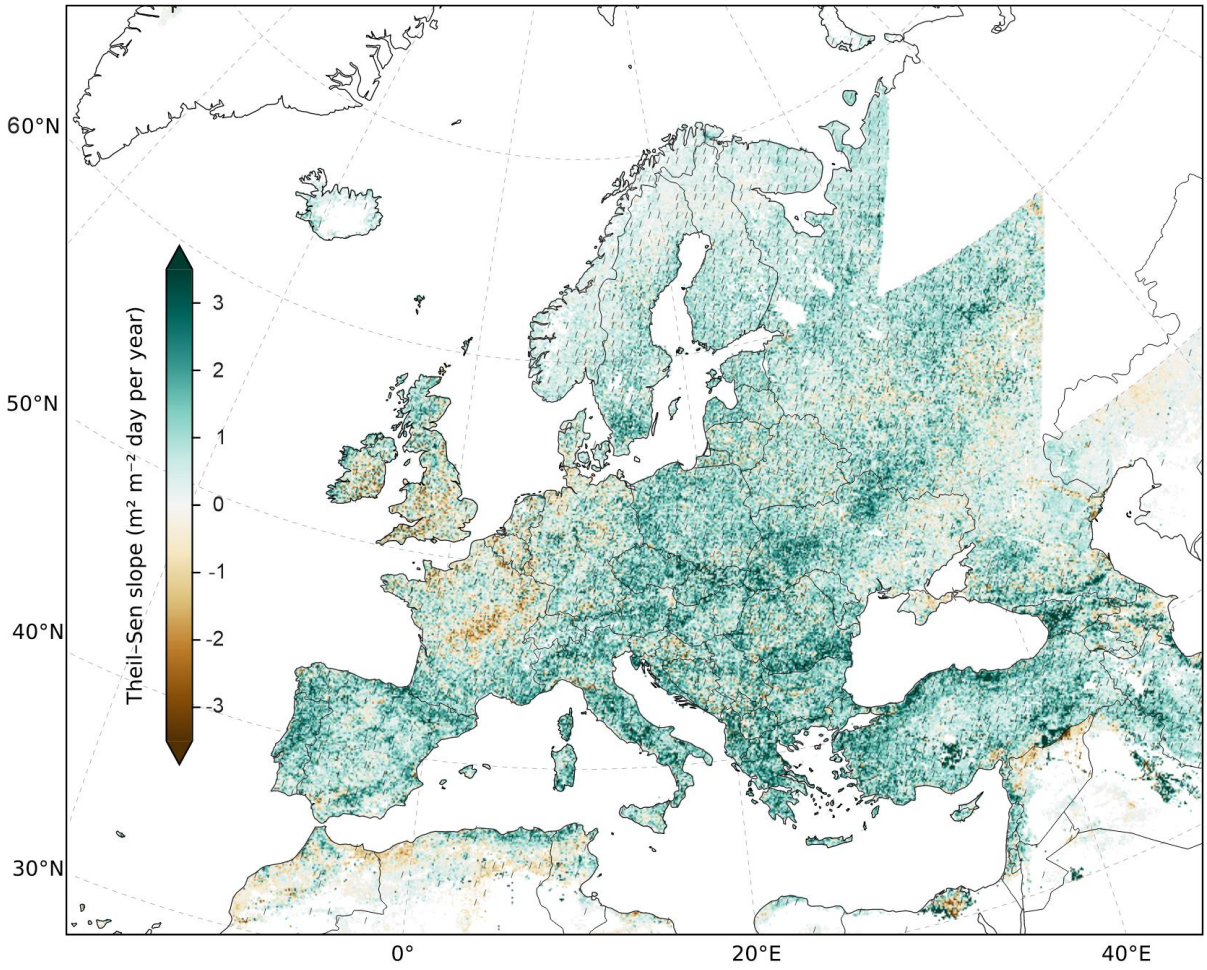


Figure 4. Theil–Sen trends in Season 1 total productivity (TPROD) across Europe, 2000–2025, derived from the 500 m MODIS-based MR-VPP 5.0 record. Brown and green indicate decreasing and increasing seasonal integrated vegetation activity, respectively. Slash symbols indicate sampled locations with Mann–Kendall $p \leq 0.05$, displayed on a regular grid at approximately 50 km spacing.

Artefact checks

Version 5.0 incorporates screening based on red reflectance and DVI to reduce false seasonality and associated high-TPROD artefacts over bright barren surfaces observed in the previous version (not publicly released; available only on request). Visual inspection included selected dryland areas (Figure 3) and volcanic terrain in the Canary Islands (not shown here).

Figure 5 compares 2025 Season 1 TPROD around Ksar Tazougart in southeastern Morocco, outside the official product coverage, with a Sentinel-2 maximum-NDVI false-color composite. Elevated TPROD broadly corresponds to cultivated areas appearing red in the composite, although not all red areas have TPROD values displayed. Exact correspondence is not expected: the datasets differ in spatial resolution, and the composite represents each pixel at its maximum observed NDVI, whereas TPROD integrates fitted PPI over a detected season. A brief greenness peak may therefore appear prominently in the

237 composite without meeting the requirements for seasonal retrieval. Missing retrievals and QA screening
238 can also contribute to differences between the panels.

239 Non-zero TPROD also occurs along apparently barren dry riverbeds. These signals may represent
240 seasonal vegetation growth or residual artefacts; the composite alone cannot distinguish between these
241 explanations. A visual comparison with the 2025 MODIS MCD12Q2 [28] phenology layers for both
242 seasons showed almost no corresponding retrievals across the inspected area, including cultivated areas
243 and dry riverbeds. In contrast, VIIRS VNP22Q2 [29] showed retrievals in cultivated areas and localized
244 patches along dry riverbeds. The Season 1 comparisons are shown in Figure 5c,d. Within the inspected
245 area, MR-VPP 5.0 therefore showed greater qualitative agreement with VNP22Q2 than with MCD12Q2
246 in the spatial occurrence of vegetation area retrievals. This pattern was observed despite MR-VPP and
247 MCD12Q2 both using MODIS NBAR inputs, and VNP22Q2 and MCD12Q2 both using the two-band
248 Enhanced Vegetation Index (EVI2)[30] as vegetation indicator. These comparisons concern retrieval
249 occurrence instead of agreement in metric magnitude, phenological timing or retrieval accuracy. Further
250 independent validation is needed to assess retrieval reliability in these dryland environments.

251 *Consistency of the 2025 annual-update window*

252 The 2025 metrics generated using a shortened processing window (1 January 2024–19 April 2026) were
253 compared pixel by pixel with those generated using the full processing record (2000–19 April 2026).
254 All processing settings were identical between the short and long tine series; only the temporal extent
255 of the input record differed. A shorter input record reduces the computational requirements of annual
256 updates, particularly for global products with large data volumes. This comparison assessed whether
257 processing the target year together with one preceding year and few subsequent months produced
258 metrics consistent with those obtained using the full record.

259 The evaluation included paired pixels in vegetated IGBP classes 1–14 using MCD12Q1 V6.1[28], with
260 QA < 127 in both outputs. Across the pan-European region, comparisons of the 13 metrics included 4.4
261 $\times 10^7$ pixel pairs for Season 1 and 6.6×10^4 for Season 2. Season 1 showed close correspondence to the
262 1:1 line, with linear-regression R^2 values of 0.97–1.00 across the 13 metrics. Mean absolute differences
263 were 0.16 days for SOSD, 0.52 days for EOSD and 0.21 $m^2\ m^{-2}$ day for TPROD. Differences were
264 larger for Season 2 EOSD and LENGTH, with mean absolute differences of 7.29 and 7.55 days,
265 respectively.

266 These results support the use of the shortened window for the evaluated 2025 annual update, particularly
267 for Season 1, while indicating greater sensitivity of secondary-season end dates and duration to the
268 temporal extent of the processing record. Full comparison results are provided in ATBD Appendix 6.3.

269

Representative PPI time series

Figure 6 presents PPI time series trajectory for individual 500 m pixels in birch forest in Abisko, Sweden; pine forest at Hyytiälä, Finland (FI-Hyy); and two pine-forest sites in northern and southern Rhodes, Greece. These examples examine the correspondence between changes in PPI and documented disturbances, illustrating seasonal development, interannual variability and subsequent recovery.

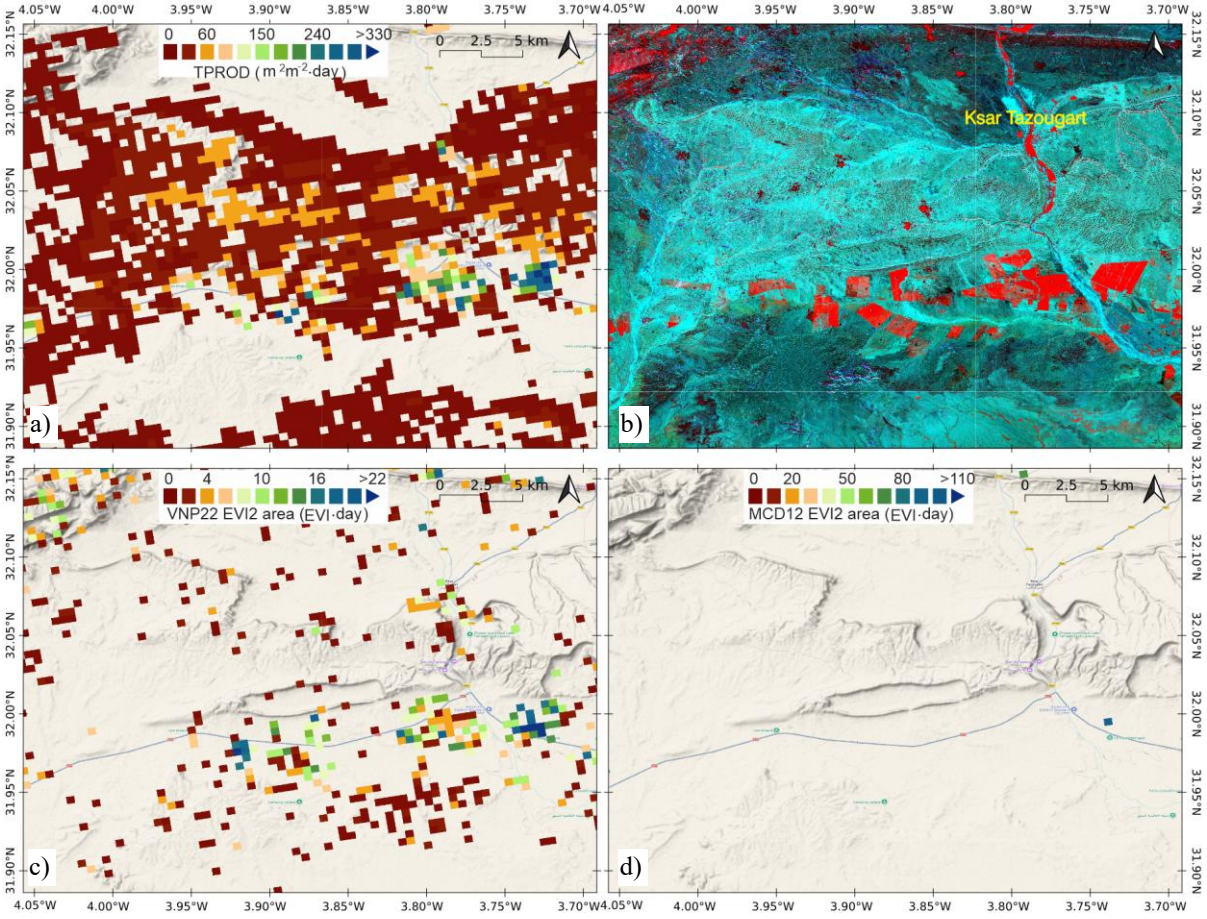


Figure 5. Comparison of (a) MR-VPP 5.0 Season 1 total productivity (TPROD), (b) a Sentinel-2 maximum-NDVI false-color composite, (c) VIIRS VNP22Q2 Season 1 EVI2 area, and (d) MODIS MCD12Q2 Season 1 EVI2 area around Ksar Tazougart, southeastern Morocco, on the northern fringe of the Sahara Desert in 2025. TPROD is displayed using the same visualization settings and QA screening as in Figure 2. The VNP22 and MCD12 EVI2 area layers show all pixels with valid retrievals. The composite assigns near-infrared (B8), green (B3) and blue (B2) reflectances to the red, green and blue display channels, respectively, using the observation with the highest NDVI at each pixel during November 2024–July 2025. Vegetated areas generally appear red. Panels (a), (c) and (d) use separate colour scales; their metric magnitudes are not directly comparable, even though (c) and (d) have same unit EVI·day.

At Abisko, reduced seasonal PPI peaks coincide with the marked insect outbreaks in 2004, 2013 and 2023, followed by higher peaks in subsequent years. This pattern is consistent with documented birch

defoliation and subsequent recovery of canopy activity [31-33]. At FI-Hyy, the seasonal PPI peak is lower in the marked 2018 drought year than in the adjacent years. The northern Rhodes series likewise shows reduced seasonal peaks around the marked periods of water stress. SPEI at the 12-month accumulation timescale (SPEI12), obtained from the Lund University Global Drought Dataset (LUGD)[34], provides meteorological context. Because SPEI12 integrates conditions over the preceding 12 months, its timing need not coincide exactly with the onset of a PPI decline. Vegetation responses also depend on when water stress occurs within the seasonal cycle.

At the southern Rhodes site, PPI declines abruptly around the 2008 and 2023 wildfires, followed by periods of low values and subsequent increases. These fires are independently documented [35,36]. Together, these examples show temporal correspondence between PPI changes and documented disturbances, supporting the use of the record to examine disturbance responses and recovery. They assess the plausibility of vegetation dynamics rather than quantify retrieval accuracy against field measurements.

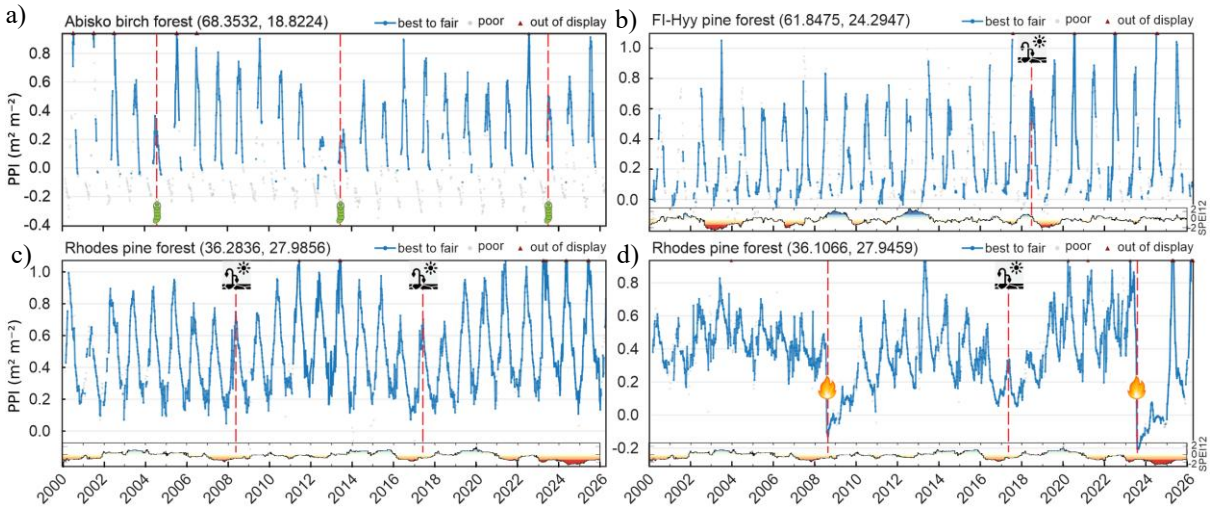


Figure 6. PPI seasonal trajectories for individual 500 m pixels at (a) birch forest in Abisko, Sweden; (b) Hyytiälä pine forest, Finland (FI-Hyy); (c) northern Rhodes pine forest, Greece; and (d) a fire-affected pine-forest site in southern Rhodes, Greece. Coordinates are given in the panel titles. Blue points and connecting lines show observations with PPI QA < 3, and grey points show observations with QA ≥ 3. Red triangles mark values outside the displayed PPI range. Red dashed lines and symbols indicate selected disturbance events discussed in the text. The lower strips in panels (b–d) show SPEI12 from LUGD; negative and positive values are shaded in orange and blue, respectively.

Usage Notes

Metric rasters are used together with their corresponding season-specific quality-assurance (QA) layers. The QA byte contains four two-bit fields: overall quality in bits 7–6, end-of-season quality in bits 5–4, peak quality in bits 3–2, and start-of-season quality in bits 1–0.

These can be decoded using `(QA >> 6) & 3`, `(QA >> 4) & 3`, `(QA >> 2) & 3`, and `QA & 3`, respectively. Each field ranges from 0 to 3, corresponding to Best, Good, Fair and Poor quality.

QA < 127 is the recommended general screen for overall Best and Good retrievals. Overall Best and Good retrievals may nevertheless contain one Poor phase, so users should decode the phase-specific quality flags when analyzing individual phenological phases. Overall Fair retrievals contain two Poor phases and may remain useful for parameters associated with the remaining adequately observed phase. Parameters spanning multiple phases, including LENGTH, LSLOPE, RSLOPE, TPROD and SPROD, require consideration of all contributing phases.

Observations before and after the target year contribute to trajectory fitting. The annual-update comparison demonstrates close agreement between shortened-window and full-record processing, with greater sensitivity in secondary-season timing. Users comparing releases should therefore consider product version, input temporal coverage and QA, particularly for seasons crossing calendar-year boundaries. Missing retrievals may reflect insufficient observational support; greater completeness alone does not imply greater accuracy.

The 500 m grid is suited to regional and continental applications. Pixels may mix vegetation types, fields, management regimes and non-vegetated surfaces, particularly near land-cover boundaries and in fragmented agricultural landscapes. When combining MR-VPP with other spatial datasets, users should align layers to a common grid and document the resampling procedure. Nearest-neighbor resampling preserves packed QA codes. Resampling of dates and continuous magnitude or productivity metrics should be selected according to the analytical objective.

At high latitudes, snow cover, low solar elevation, polar night and insufficient BRDF retrievals may limit observational support. Gap treatment supports curve fitting but may affect estimates of SOSD, EOSD and LENGTH and reduce sensitivity to weak winter activity. Weakly seasonal evergreen vegetation and sparsely vegetated surfaces also require cautious interpretation.

Data Availability

Data availability and download access points are listed in Table 2. Downloading requires an EU Login, the European Commission's user authentication service for accessing its web services. Product technical support is provided by the product custodian through the Copernicus Land Monitoring Service helpdesk: copernicus@eea.europa.eu.

Code Availability

Code can be shared upon reasonable requirements. Core scripts of TIMESAT Version 4.2 for trajectory fitting and metric extraction is available at https://github.com/TIMESAT.

Acknowledgements

The Medium Resolution Vegetation Phenology and Productivity (MR-VPP) dataset was produced for the European Environment Agency (EEA) under the Copernicus Land Monitoring Service (CLMS) by the Flemish Institute for Technological Research (VITO), with contributions from Lund University led by LE. Data processing and demonstration analyses were carried out using LUNARC high-performance computing resources, provided through the National Academic Infrastructure for Supercomputing in Sweden (NAISS). The authors also acknowledge open-access publishing support from Lund University.

Funding

European Environment Agency (EEA) contract No EEA/DIS/R0/23/007 – Lot 1, contracted with VITO and with contribution by Lund University led by LE. HJ and ZC were partly funded by the EU Horizon project BioClima (grant agreement No. 101181408). Computing was additionally supported by an infrastructure grant awarded to JA by the Faculty of Science at Lund University.

Author Contributions

EI proposed and initiated the first version of the dataset. LF and LB subsequently served as MR-VPP project officers. HJ designed the processing chain for MR-VPP 5.0, performed data processing, quality checks and validation, and drafted the manuscript. ZC implemented TIMESAT Version 4.2. AV, DDM, ES, WH, WTN and DB coordinated product implementation and reporting under the service contract. JA secured funds for computing facilities. LE led the Lund University team's contribution. All authors reviewed and approved the Data Descriptor.

Competing Interests

The authors declare no competing interests.

AI usage

OpenAI GPT-6.1 Sol was used to assist with literature searches, checks of manuscript conformity with journal requirements, and improvements to language and readability. It was also used through Codex to assist with preliminary checks of data and figures. The authors reviewed and verified all AI-assisted

outputs and retained full intellectual control and final decision-making authority over the study's content, algorithms, analyses, figures and conclusions. The authors take full responsibility for the accuracy, integrity and originality of the work.

References

1 Lieth, H. Phenology and Seasonality Modeling (Ecological Studies-Analysis and Synthesis Series, Vol 8). 444 (1974). https://doi.org/10.1007/978-3-642-51863-8

2 de Beurs, K. M. & Henebry, G. M. Land surface phenology, climatic variation, and institutional change: Analyzing agricultural land cover change in Kazakhstan. *Remote Sensing of Environment* **89**, 497-509 (2004). http://dx.doi.org/10.1016/j.rse.2003.11.006

3 White, M. A. *et al.* Intercomparison, interpretation, and assessment of spring phenology in North America estimated from remote sensing for 1982–2006. *Global Change Biology* **15**, 2335-2359 (2009). http://dx.doi.org/10.1111/j.1365-2486.2009.01910.x

4 Friedl, M. *et al. Land surface phenology*, <http://landportal.gsfc.nasa.gov/Documents/ESDR/Phenology_Friedl_whitepaper.pdf> (2006).

5 Schwartz, M. D. Phenology: An Integrative Environmental Science 644 (2024). https://doi.org/10.1007/978-3-031-75027-4

6 Jin, H. *et al.* Higher vegetation sensitivity to meteorological drought in autumn than spring across European biomes. *Communications Earth & Environment* **4**, 299 (2023). https://doi.org/10.1038/s43247-023-00960-w

7 Jin, H. *et al.* New satellite-based estimates show significant trends in spring phenology and complex sensitivities to temperature and precipitation at northern European latitudes. *International Journal of Biometeorology* **63**, 763–775 (2019). https://doi.org/10.1007/s00484-019-01690-5

8 Garonna, I., de Jong, R. & Schaepman, M. E. Variability and evolution of global land surface phenology over the past three decades (1982–2012). *Global Change Biology* **22**, 1456-1468 (2016). http://dx.doi.org/10.1111/gcb.13168

9 CLMS. Product update: Medium Resolution Vegetation Phenology and Productivity Version 5.0. https://land.copernicus.eu/en/news/product-update-medium-resolution-vegetation-phenology-and-productivity-version-5.0. (2026).

10 EEA. 8th Environment Action Programme Drought impact on ecosystems in Europe 2024 https://www.eea.europa.eu/en/analysis/publications/monitoring-progress-towards-8th-eap-objectives/indicators/04-drought-impact-on-ecosystems-in-europe. (2024).

11 EEA. Annual area exposed to drought (line) and impacted by drought (bars) in the EU, 2000-2025, https://www.eea.europa.eu/en/analysis/indicators/drought-impact-on-ecosystems-in-europe/annual-area-exposed-to-drought. (2026).

12 Jin, H. & Eklundh, L. A physically based vegetation index for improved monitoring of plant phenology. *Remote Sensing of Environment* **152**, 512-525 (2014). https://doi.org/10.1016/j.rse.2014.07.010

13 Marsh, H. *et al.* Plant Phenology Index leveraging over conventional vegetation indices to establish a new remote sensing benchmark of GPP for northern ecosystems. *International Journal of Applied Earth Observation and Geoinformation* **136**, 104289 (2025). https://doi.org/10.1016/j.jag.2024.104289

14 Junttila, S. *et al.* Estimating local-scale forest GPP in Northern Europe using Sentinel-2: Model comparisons with LUE, APAR, the plant phenology index, and a light response function. *Science of Remote Sensing* **7**, 100075 (2023). https://doi.org/10.1016/j.srs.2022.100075

15 Abdi, A. M. *et al.* First assessment of the plant phenology index (PPI) for estimating gross primary productivity in African semi-arid ecosystems. *International Journal of Applied Earth*

Observation and Geoinformation **78**, 249-260 (2019). https://doi.org/10.1016/j.jag.2019.01.018

16 Terasaki Hart, D. E., Bùi, T.-N., Di Maggio, L. & Wang, I. J. Global phenology maps reveal the drivers and effects of seasonal asynchrony. *Nature* **645**, 133-140 (2025). https://doi.org/10.1038/s41586-025-09410-3

17 Stocker, B. D. *et al.* Drought impacts on terrestrial primary production underestimated by satellite monitoring. *Nature Geoscience* **12**, 264-270 (2019). 10.1038/s41561-019-0318-6

18 Cai, Z., Eklundh, L. & Jönsson, P. TIMESAT4: is a software package for analysing time-series of satellite sensor data (Version 4.1.x) [Computer software]. *Zenodo* (2025). https://doi.org/10.5281/zenodo.19881054

19 CLMS. CLMS Medium Resolution Vegetation Phenology and Productivity (MR-VPP) – Algorithm Theoretical Basis Document (ATBD), https://library.land.copernicus.eu/products/MRVPP_MRVPP_ATBD_v2.html. (2026).

20 CLMS. Medium Resolution Vegetation Phenology and Productivity (MR-VPP) – Product User Manual (PUM), https://library.land.copernicus.eu/products/MRVPP_MRVPP_PUM_v1.html. (2026).

21 Schaaf, C. B. *et al.* First operational BRDF, albedo nadir reflectance products from MODIS. *Remote Sensing of Environment* **83**, 135-148 (2002). http://dx.doi.org/10.1016/S0034-4257(02)00091-3

22 Jönsson, P. & Eklundh, L. Seasonality extraction by function fitting to time-series of satellite sensor data. *Geoscience and Remote Sensing, IEEE Transactions on* **40**, 1824-1832 (2002). https://doi.org/10.1109/TGRS.2002.802519

23 Cai, Z., Jönsson, P., Jin, H. & Eklundh, L. Performance of Smoothing Methods for Reconstructing NDVI Time-Series and Estimating Vegetation Phenology from MODIS Data. *Remote Sensing* **9**, 1271 (2017). https://doi.org/10.3390/rs9121271

24 CLMS. CLMS releases the new NDVI V3: key features and user benefits. https://land.copernicus.eu/en/news/clms-releases-the-new-ndvi-v3-key-features-and-user-benefits. (2025).

25 Ciais, P. *et al.* Europe-wide reduction in primary productivity caused by the heat and drought in 2003. *Nature* **437**, 529 (2005). http://doi.org/10.1038/nature03972

26 Ionita, M. *et al.* The European 2015 drought from a climatological perspective. *Hydrol. Earth Syst. Sci.* **21**, 1397-1419 (2017). https://doi.org/10.5194/hess-21-1397-2017

27 Tian, F. *et al.* Calibrating vegetation phenology from Sentinel-2 using eddy covariance, PhenoCam, and PEP725 networks across Europe. *Remote Sensing of Environment* **260**, 112456 (2021). https://doi.org/10.1016/j.rse.2021.112456

28 Friedl, M., Gray, J. & Sulla-Menashe, D. MODIS/Terra+Aqua Land Cover Dynamics Yearly L3 Global 500m SIN Grid V061 [Dataset]. NASA Land Processes Distributed Active Archive Center. https://doi.org/10.5067/MODIS/MCD12Q2.061 Date Accessed: 2026-10-10. (2022).

29 Zhang, X. VIIRS/NPP Land Surface Phenology Yearly L3 Global 500m SIN Grid V002 [Dataset]. NASA Land Processes Distributed Active Archive Center. https://doi.org/10.5067/VIIRS/VNP22Q2.002 Date Accessed: 2026-10-10. (2024).

30 Jiang, Z., Huete, A. R., Didan, K. & Miura, T. Development of a two-band enhanced vegetation index without a blue band. *Remote Sensing of Environment* **112**, 3833-3845 (2008).

31 Heliasz, M. *et al.* Quantification of C uptake in subarctic birch forest after setback by an extreme insect outbreak. *Geophysical Research Letters* **38**, L01704 (2011). https://doi.org/10.1029/2010GL044733

32 Olsson, P.-O., Lindström, J. & Eklundh, L. Near real-time monitoring of insect induced defoliation in subalpine birch forests with MODIS derived NDVI. *Remote Sensing of Environment* **181**, 42-53 (2016). http://dx.doi.org/10.1016/j.rse.2016.03.040

33 Rieksta, J. *et al.* Insect outbreak progression over three years shapes biogenic volatile emissions in a mountain birch forest. *Communications Earth & Environment* **7**, 816 (2026). https://doi.org/10.1038/s43247-026-03920-2

34 Jin, H. Lund University Global Drought Dataset (LUGD), 1981–2025: Weekly 0.1° SPEI with Accumulation Timescales from 1 Week to 48 Months – Northern Hemisphere [Dataset]. *Zenodo* (2026). https://doi.org/10.5281/zenodo.18985819

35 JRC. Forest Fires in Europe 2008 <https://data.effis.emergency.copernicus.eu/effis/reports-and-publications/annual-fire-reports/forest-fires-in-europe-2008.pdf>. (TP261, I-21027, Ispra (VA)|, Italy, 2008).

36 Bilgehan Makineci, H. Investigation of burned areas with multiplatform remote sensing data on the Rhodes 2023 forest fires. *Ain Shams Engineering Journal* **15**, 102949 (2024). https://doi.org/10.1016/j.asej.2024.102949